The proteomics of quiescent and nonquiescent cell differentiation in yeast stationary-phase cultures

George S. Davidson[a,b], Ray M. Joe[a], Sushmita Roy[c], Osorio Meirelles[a], Chris P. Allen[d], Melissa R. Wilson[a], Phillip H. Tapia[d], Elaine E. Manzanilla[a], Anne E. Dodson[a], Swagata Chakraborty[a], Mark Carter[d], Susan Young[d], Bruce Edwards[d], Larry Sklar[d,e], and Margaret Werner-Washburne[a]

[a]Biology Department, University of New Mexico, Albuquerque, NM 87131; [b]Sandia National Laboratories, Albuquerque, NM 81185; [c]Computer Science Department, University of New Mexico, Albuquerque, NM 87131; [d]Department of Cytometry and [e]Department of Pathology, University of New Mexico School of Medicine, Albuquerque, NM 87131

ABSTRACT As yeast cultures enter stationary phase in rich, glucose-based medium, differentiation of two major subpopulations of cells, termed quiescent and nonquiescent, is observed. Differences in mRNA abundance between exponentially growing and stationary-phase cultures and quiescent and nonquiescent cells are known, but little was known about protein abundance in these cells. To measure protein abundance in exponential and stationary-phase cultures, the yeast GFP-fusion library (4159 strains) was examined during exponential and stationary phases, using high-throughput flow cytometry (HyperCyt). Approximately 5% of proteins in the library showed twofold or greater changes in median fluorescence intensity (abundance) between the two conditions. We examined 38 strains exhibiting two distinct fluorescence-intensity peaks in stationary phase and determined that the two fluorescence peaks distinguished quiescent and nonquiescent cells, the two major subpopulations of cells in stationary-phase cultures. GFP-fusion proteins in this group were more abundant in quiescent cells, and half were involved in mitochondrial function, consistent with the sixfold increase in respiration observed in quiescent cells and the relative absence of Cit1p:GFP in nonquiescent cells. Finally, examination of quiescent cell–specific GFP-fusion proteins revealed symmetry in protein accumulation in dividing quiescent and nonquiescent cells after glucose exhaustion, leading to a new model for the differentiation of these cells.

Monitoring Editor
Thomas D. Fox
Cornell University

Received: Jun 9, 2010
Revised: Jan 6, 2011
Accepted: Jan 19, 2011

INTRODUCTION

The yeast *Saccharomyces cerevisiae* is a major model system that is seldom considered for studies of cellular differentiation, especially the differentiation of cell types within the same culture. However, when yeast cultures, grown in rich, glucose-based medium, exhaust glucose, two cell fractions—quiescent (Q) and nonquiescent (NQ)—do differentiate and, by 2 d after glucose exhaustion (3 d after inoculation), are separable by density-gradient centrifugation (Allen *et al.*, 2006).

We called the dense cells "quiescent" because they are long lived (Li *et al.*, 2009), stress resistant, and uniform and retain the capacity to respond in different ways to the environment (Allen *et al.*, 2006). Q cells are also unbudded, bright (refractile) by phase-contrast microscopy, and relatively dense, and most (>90%) are virgin daughters. They are synchronous when refed and nearly 100% reproductively competent. They contain thousands of mRNAs in insoluble protein–RNA complexes from which specific mRNAs are released in a stress-specific manner (Aragon *et al.*, 2006), and the mRNAs that are abundant in these cells include many signaling molecules needed for progrowth responses (Aragon *et al.*, 2008).

The NQ fraction, in contrast, is heterogeneous and retains viability but rapidly loses the ability to reproduce, suggesting that NQ cells

This article was published online ahead of print in MBoC in Press (http://www.molbiolcell.org/cgi/doi/10.1091/mbc.E10-06-0499) on February 2, 2011.

Address correspondence to: Margaret Werner-Washburne (maggieww@unm.edu).

Abbreviations used: CFU, colony-forming unit; DHE, dihydroethidium; EFα, elongation factor α; EXP, exponential growth phase; GFP, green fluorescent protein; GO, gene ontology; NQ, nonquiescent; PBS, phosphate-buffered saline; Q, quiescent; ROS, reactive oxygen species; SDI, slope-differentiation identification; SP, stationary phase; YPD, yeast peptone dextrose.

are in a terminal state and may be a model for the "viable but unculturable" state of most microbes in the environment (Lewis, 2007). The NQ fraction contains budded and unbudded cells composed of approximately equal numbers of mothers and daughters and contain few sequestered mRNAs. This fraction is not synchronous when refed and, of the NQ cells that can reproduce, 40% form petite colonies, consistent with previous reports of genomic rearrangements and transpositions in stationary phase (SP) or glucose-limited cultures (Dunham *et al.*, 2002; Coyle and Kroll, 2008). The most abundant, soluble mRNAs in NQ cells encode proteins involved in DNA recombination and repair and Ty-element transposition, consistent with genomic instability (Aragon *et al.*, 2008). By 14 d postinoculation, ~50% of NQ cells exhibit signs of apoptosis (Allen *et al.*, 2006). The differences between Q and NQ cells and the preponderance of Q cells that are virgin daughters raise questions about the origins and the regulation of the differentiation of these populations.

Large, robust transcriptome data sets are available for Q and NQ cells (Aragon *et al.*, 2008), but no extensive proteomic data are available for these fractions. Before this article, the only proteomic data available were from two-dimensional polyacrylamide gel electrophoretograms from studies of protein synthesis in cultures grown to SP in rich medium (Fuge *et al.*, 1994). This analysis demonstrated that, although protein synthesis decreases as cultures approached SP, there are major changes in protein synthesis immediately after the cultures exhaust glucose at the diauxic shift.

To obtain quantitative data for abundance of more than two-thirds of yeast proteins, the yeast green fluorescent protein (GFP)–fusion library (4159 strains, each tagged at the 3′ end of the open reading frame with a GFP-encoding gene) (Huh *et al.*, 2003) was screened, in triplicate, during exponential phase (EXP) and SP, using high-throughput flow cytometry (HyperCyt) (Edwards *et al.*, 2004). The GFP-fusion library was developed as a tool for in vivo analysis of protein abundance and localization at the level of the proteome. The strain library, which represents ~75% of all yeast genes, has been validated and used to localize proteins in cells in EXP cultures. It has also been used to examine the relationship between mRNA and protein abundance (Newman *et al.*, 2006), and this and similar libraries have been used to model the factors that contribute to differences in protein abundance at the cellular level (Raser and O'Shea, 2004, 2005; Newman *et al.*, 2006). However, to our knowledge, the entire library has not previously been used to examine differences in protein abundance between two environmental conditions, such as EXP in rich, glucose-based medium and SP.

We report here from flow-cytometry analysis of ~25,000 samples from the GFP-fusion strains in EXP and SP that 5% of GFP-fusion proteins showed a twofold or greater change in abundance between EXP and SP. Abundant EXP proteins are involved in biosynthetic processes while abundant SP proteins are involved in mitochondrial function. To find GFP-fusion proteins that might distinguish Q from NQ cells, we identified 38 strains with distinct double peaks of fluorescence in unfractionated SP cultures. All 38 strains exhibited higher fluorescence intensity in the Q fraction. Most of these strains carried GFP fusions in mitochondrial proteins, many of which are involved in respiration. This unexpected observation was corroborated by our finding that respiration was significantly higher in Q than NQ cells. Examination of Cit1p:GFP and Acs1p:GFP strains, which express GFP-fusion proteins almost exclusively in Q cells, revealed that daughter cells produced after the diauxic shift express the same level of GFP protein as the mother; that is, dim NQ mothers produce dim NQ daughters while bright, GFP-producing mothers produce bright daughters. These observations led to a new model for the production of Q and NQ cells in SP cultures.

RESULTS

Assay of the yeast GFP-fusion library in EXP and SP provided new insights into the EXP-to-SP transition

Previously, the only information about protein abundance as cells transition from EXP to SP came from two-dimensional gel analysis of radioactively labeled and unlabeled proteins (Fuge *et al.*, 1994). To better quantify the change in protein abundance between these phases, we analyzed the yeast GFP-fusion library (4159 strains, each carrying the GFP gene inserted into a known 3′ region of a different gene and under the control of a native promoter) (Huh *et al.*, 2003) and the HyperCyt high-throughput flow cytometer (Edwards *et al.*, 2004). All samples were assayed in triplicate under the two conditions (~25,000 samples).

Fluorescence measurements in EXP and SP samples were extremely robust ($R^2 = 0.995$) for 96-well plates containing the same strains sampled more than a month apart (see Supplemental Material). Previous studies, using an identical GFP fusion set, reported similar reproducibility ($R^2 = 0.997$), that is, measurement reproducibility between replicate experiments in the same laboratory (Newman *et al.*, 2006). Comparison of the abundance of 2735 proteins between our results and those of Newman *et al.* gave a Pearson's $R = 0.91$, indicating that reproducibility between laboratories is also excellent and, thus, that measured protein expression in the library under similar conditions is highly reproducible. Newman found that GFP measurements and tandem affinity purification–tag measurements for those proteins were closely correlated ($R^2 = 0.80$) and were comparable to the precision achieved with duplicate Western blots ($R^2 = 0.77$). Thus there is strong evidence that GFP intensity is a true measure of protein abundance for these fusion proteins.

Of the top 20 most abundant proteins in EXP and SP, 12 were abundant under both conditions (Table 1). These proteins are involved in glycolysis (5 proteins), cell wall biosynthesis (1), translation (including the two translation elongation factors Tef1p and Tef2p, which both encode elongation factor α [EFα] [Schirmaier and Philippsen, 1984] and Yef3p [Qin *et al.*, 1987]), protein translation, folding, stability, and transport into various organelles (Ssa1p and Ssa2p [Deshaies *et al.*, 1988; Horton *et al.*, 2001] and Hsc82p, involved in proteasome assembly [Imai *et al.*, 2003; Le Tallec *et al.*, 2007]). Proteins that were among the 20 most abundant in EXP but not in SP were Ahp1p, a thiol-specific peroxiredoxin that protects against oxidative damage (Lee *et al.*, 1999), and 3 proteins that are part of the ribosomal stalk (Table 1). Also included were Pgi1p, which catalyzes the interconversion of glucose-6-phosphate and fructose-6-phosphate and is required for cell cycle progression (Dickinson, 1991), and Pfk2p, a subunit of phosphofructokinase that is required for glucose induction of cell cycle–related genes (Aguilera, 1986). Gene ontology (GO) analysis for proteins with high abundance in EXP were involved in biosynthetic processes, especially translation (40%) (Table 2; Supplemental Material).

Proteins abundant in SP (Table 1) were typically associated with aging and stress phenotypes, including two ribosomal large-subunit proteins associated with increased fitness (Rpl41a and Rpl22a) (Planta and Mager, 1998; Giaever *et al.*, 2002). Abundant proteins were also involved in an NADPH-generating step of the pentose phosphate pathway (Gnd1p), which is required for resistance to oxidative stress (Izawa *et al.*, 1998), and glucose kinase (Hxk2p), which is required for competitive fitness and growth on fermentable carbon sources (Kaeberlein *et al.*, 2005). Finally, abundant proteins included the vacuolar ATPase (Tfp1p), required for

Gene name	Std name	Function	Log_2EXP	Log_2SP
YLR044C	*PDC1*	Pyruvate decarboxylase	10.39	8.41
YHR174W	*ENO2*	Enolase II, a phosphopyruvate hydratase	10.12	9.47
YGR192C	*TDH3*	Glyceraldehyde-3-phosphate dehydrogenase	10.01	8.75
YKL060C	*FBA1*	Fructose 1,6-bisphosphate aldolase	9.97	8.42
YPR080W	*TEF1*	Translational elongation factor EF1α	9.16	8.34
YLL024C	*SSA2*	ATP binding protein	9.16	8.24
YBR118W	*TEF2*	Translational elongation factor EF1α	9.09	7.81
YJR009C	*TDH2*	Glyceraldehyde-3-phosphate dehydrogenase	8.91	7.59
YAL005C	*SSA1*	ATPase	8.71	9.05
YLR249W	*YEF3*	Translational elongation factor 3	8.54	6.62
YDL055C	*PSA1*	GDP-mannose pyrophosphorylase	8.5	6.47
YMR186W	*HSC82*	Cytoplasmic chaperone of the Hsp90 family	8.49	6.85
YLR109W	*AHP1*	Thiol-specific peroxiredoxin	8.23	5.78
YBR196C	*PGI1*	Glycolytic enzyme phosphoglucose isomerase	7.7	5.64
YMR205C	*PFK2*	Beta subunit of hetero-octameric phosphofructokinase	7.66	6.16
YDR382W	*RPP2B*	Ribosomal protein P2 beta	7.52	6.1
YDL130W	*RPP1B*	Ribosomal protein P1 beta	7.5	5.66
YDL081C	*RPP1A*	Ribosomal stalk protein P1 alpha	7.42	6.08
YBR189W	*RPS9B*	Protein component of the small (40S) ribosomal subunit	7.32	5.98
YGL135W	*RPL1B*	N-terminally acetylated protein component of the large (60S) ribosomal subunit	7.33	5.76
YGL253W	*HXK2*	Hexokinase isoenzyme 2	6.97	7.04
YDR070C	*FMP16*	Putative protein of unknown function	4.43	6.9
YDL185W	*TFP1*	The A subunit of the V-ATPase V1 domain	6.73	6.74
YJL138C	*TIF2*	Translation initiation factor eIF4A	6.83	6.61
YDL184C	*RPL41A*	Ribosomal protein L47 of the large (60S) ribosomal subunit	6.74	6.55
YFL014W	*HSP12*	Protein that protects membranes from desiccation	3.89	6.54
YLR061W	*RPL22A*	Protein component of the large (60S) ribosomal subunit	6.62	6.54
YHR183W	*GND1*	6-Phosphogluconate dehydrogenase (decarboxylating)	6.27	6.5

TABLE 1: Most abundant proteins in EXP and SP.

resistance to a variety of stresses (Stevens and Forgac, 1997), and the translation initiation factor eIF4a (Tif2p), a DEAD/DEAH-box RNA helicase that is a current target for cancer therapeutics (Lindqvist and Pelletier, 2009; Li *et al.*, 2010). This is consistent with the hypothesis that a major role for SP proteins is in stress resistance.

Although cells undergo a major metabolic shift during the transition from 2% glucose to essentially no fermentable carbon between EXP and SP, only 5% of the 4159 GFP-fusion proteins showed ≥twofold changes in abundance: with 121 proteins more abundant in EXP and 87 more abundant in SP (Figure 1). Interestingly, proteins that showed large increases in abundance in cells in SP cultures compared with EXP cultures were typically low-abundance proteins in EXP, while many of the proteins with significant increases in abundance in EXP compared with SP were relatively high-abundance in cells under both conditions. Because ~1800 GFP fusions that did not give a signal in EXP were eliminated from the library (Huh *et al.*, 2003), many strains that express GFP-fusion protein in SP may be absent. A lower percentage of proteins with twofold or higher abundance in EXP had unknown functions (4 of 121 or 3.3%) than those proteins high in SP (21 of 87 or 24.1%). We conclude from these results that relatively few major changes in protein abundance occur during the EXP-to-SP transition. Second, because SP-abundant proteins are typically low-abundance proteins in EXP, survival in SP may require new and, in some cases, previously unstudied processes, consistent with the relatively understudied nature of this part of the yeast life cycle.

GO analyses revealed that proteins increasing at least twofold in SP cultures were involved in respiration, including ATP synthesis and electron transport (Table 2; Supplemental Material). Nine proteins involved in stress response, primarily oxidative stress, were identified, including Hsp12p and the two superoxide dismutases Sod1p and Sod2p (Auesukaree *et al.*, 2009). A similar number of proteins were involved in chromatin silencing, modification, and histone acetylation (see Supplemental Material). These results are consistent with previous findings that mitochondrial function is important for Q cell survival and that Q cells are stress resistant and genomically stable (Allen *et al.*, 2006; Aragon *et al.*, 2008).

Processes for proteins	Proteins in each GO category	P-value
Expressed in SP		
Oxidative phosphorylation	11	2.8×10^{-9}
Generation of precursor metabolites and energy	17	1.2×10^{-6}
Electron transport chain	8	1.4×10^{-6}
Respiratory electron transport chain	8	1.4×10^{-6}
ATP synthesis coupled electron transport	8	1.4×10^{-6}
Mitochondrial ATP synthesis coupled electron transport	8	1.4×10^{-6}
Oxidation reduction	8	1.4×10^{-6}
Cofactor metabolic process	16	5.2×10^{-6}
Expressed in EXP		
Translation	49	5.5×10^{-22}
Biosynthetic process	79	4.1×10^{-11}
Cellular protein metabolic process	62	1.7×10^{-10}
Protein metabolic process	63	3.0×10^{-10}
Cellular biosynthetic process	74	7.6×10^{-9}
Primary metabolic process	98	4.2×10^{-7}

TABLE 2: GO process of proteins expressed twofold or higher in SP (87 proteins) or EXP (121 proteins).

Identification and characterization of strains exhibiting two fluorescent populations in SP cultures identified differences between Q and NQ cells

We have shown previously that there are two major cellular fractions in SP cultures: Q and NQ (Allen *et al.*, 2006). In a microscopic examination of highly fluorescent strains, Cit1p:GFP, encoding citrate synthase (Suissa *et al.*, 1984; Kim *et al.*, 1986), clearly exhibited two

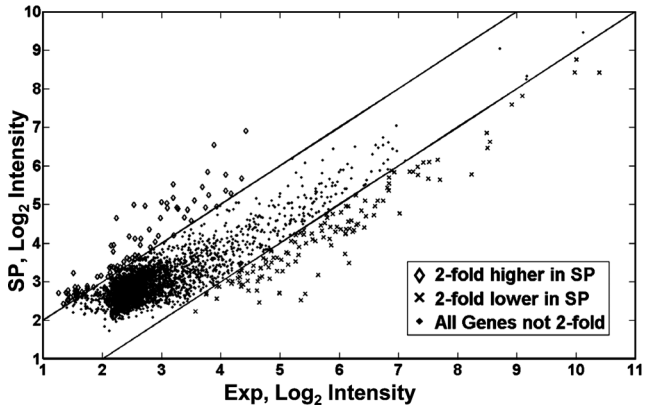

FIGURE 1. EXP and SP distributions of median peak intensities measured by high-throughput flow cytometry for strains from the yeast GFP-fusion library in EXP and SP. Points outside the diagonal, parallel lines identify strains whose differences between SP and EXP are greater than twofold. A list of these genes can be found in the Supplemental Material. (◊) 87 GFP-fusion proteins with twofold or greater increases in SP phase. (X) 121 GFP-fusion proteins with twofold or greater increases in EXP phase.

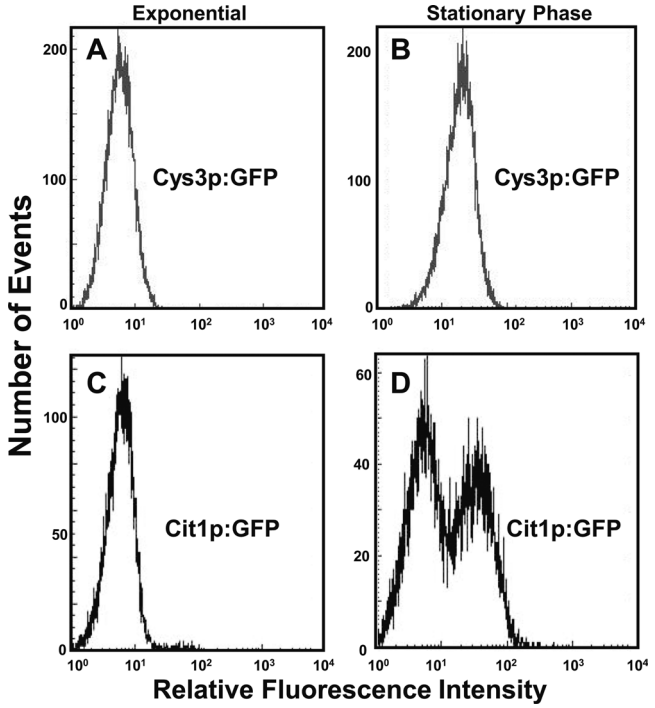

FIGURE 2: Histogram of fluorescence-intensity distributions for Cys3p:GFP and Cit1p:GFP fusion strains from EXP and unfractionated SP cultures. Flow-cytometry measurements were collected as described in *Materials and Methods*.

populations of cells in SP but not in EXP (Figure 2D). Examination of NQ and Q cells from SP cultures by flow cytometry clearly showed greater abundance of Cit1p:GFP in the Q fraction (Figure 3). There was no free GFP observed by Western blot using anti-GFP antibody, indicating that all GFP was found in the Cit1p:GFP construct (see Supplemental Material). We determined, using the MoFlo cell sorter, that the reproductive capacity and petite formation of Cit1p:GFP-producing cells were essentially identical to that of Q cells and dim Cit1p:GFP cells were similar to the NQ fraction (see Supplemental Material). Thus we concluded that Cit1p:GFP expression can be used as a surrogate to identify cells with characteristics of Q cells, which are found predominately in the Q fraction and to a much smaller extent in the less-dense NQ fraction.

We used three different methods to identify strains with two peaks of fluorescence intensity: visual evaluation of the flow-cytometry output for 4159 of ~12,500 samples, k-means clustering, and a statistical method we called slope-differentiation identification (SDI) (see *Materials and Methods*). Thirty-eight strains were predicted by all three methods to have multiple intensity peaks and were examined further.

Microscopic evaluation revealed that, in all 38 strains exhibiting two peaks of fluorescence, GFP-fusion proteins were more abundant in Q cells

Flow-cytometry measurements of Q:NQ median fluorescence ratios ranged from 37 for cytoplasmic Hsp12p:GFP, which is involved oxidative stress resistance and in membrane stabilization during desiccation (Sales *et al.*, 2000), to 1.4 for Cox6p:GFP, a cytochrome *c* oxidase protein (Wright *et al.*, 1995) (Figure 4). Twenty of the 38 GFP-fusion proteins were localized to the mitochondria, and most of those with Q:NQ fluorescence ratios ≥5 were localized to the mitochondria. Nonmitochondrial GFP-fusion proteins with high Q:NQ

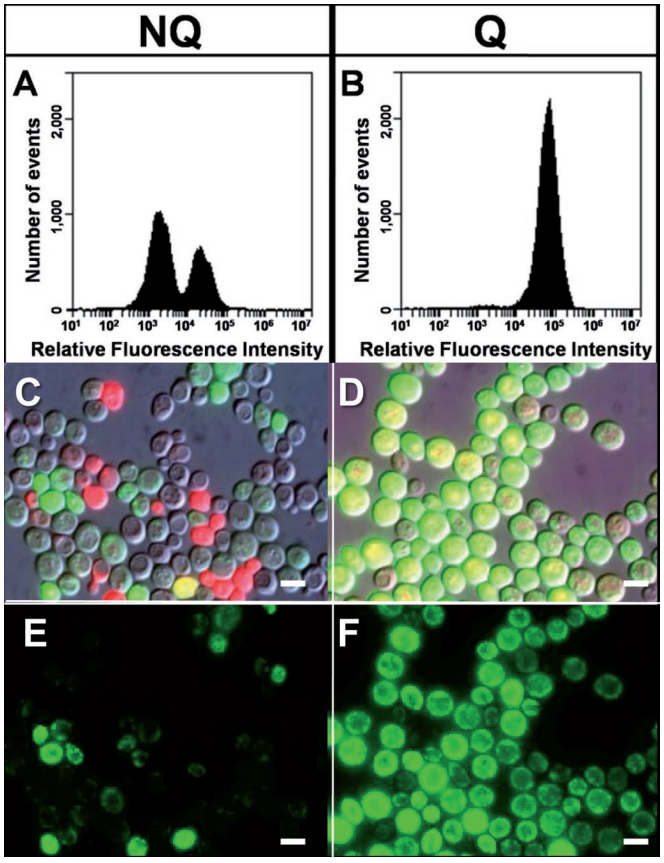

FIGURE 3: Distribution of Cit1p:GFP fluorescence intensity in fractionated Q and NQ populations as detected by flow cytometry and microscopy. (A) Cit1p:GFP fluorescence-intensity histogram for the NQ fraction. (B) GFP fluorescence-intensity histogram for the Q fraction. (C and E) NQ fraction of Cit1p:GFP stained with DHE (red) indicating reactive oxygen stress. (E) Cit1p:GFP alone for the NQ fraction in C. (D and F) Q fraction. (D) Q fraction of Cit1p:GFP cells stained with DHE, indicating ROS. (F) Corresponding micrograph showing Cit1p:GFP for Q cells. (C–F) White scale bars are 5 μm.

fluorescence ratios included the heat shock protein Hsp12p; acetyl CoA synthetase, involved in histone acetylation (Acs1P) (DeVirgilio *et al.*, 1992); and Nce102p, a putative membrane protein of unknown function that associates with lipid rafts and is involved in secretion of proteins with nonclassical signal sequences (Bagnat *et al.*, 2000). Another protein, Inh1p, is an ATPase inhibitor with typical mitochondrial localization, suggesting that, while mitochondrial profiles in Q cells are robust, ATPase function may be inhibited. We conclude from these results that abundant proteins in Q cells are consistent with mitochondrial maintenance and long-term survival and that the changes in protein abundance observed in unfractionated SP cultures reflect the change in protein abundance in Q cells.

In the evaluation of separated Q and NQ fractions from the 38 strains described above, 29 of the 38 strains, carrying mostly GFP fusions uniquely localized to the mitochondria (Figure 4), showed two peaks of fluorescence intensity in the NQ fraction (see Supplemental Material). These strains typically had a larger low-fluorescence peak and a smaller higher-fluorescence peak, at slightly lower fluorescence intensity than the Q cell fraction (Figure 3). This is consistent with several observations of heterogeneity in the NQ fraction, including reactive oxygen species (ROS) accumulation and reproductive capacity (Allen *et al.*, 2006).

To characterize the subpopulations in NQ fractions, we examined several strains, including Kgd1p:GFP, a component of α-ketoglutarate dehydrogenase (Repetto and Tzagoloff, 1989); Fmp16p:GFP, a mitochondrial protein of unknown function (Reinders *et al.*, 2006); Eno1p:GFP, cytoplasmic enolase (McAlister and Holland, 1982); Sbp1p:GFP, an RNA-binding protein (Segal *et al.*, 2006); and Ndi1p:GFP, NADH:ubiquinone oxidoreductase (Li *et al.*, 2006). To identify cells with ROS, NQ fractions were also stained with dihydroethidium (DHE). Before sorting, three subpopulations were observed in NQ fractions: cells with low GFP and high ROS, cells with high GFP and low ROS, and cells with both low GFP and low ROS (Figure 3C). No cells with both high ROS and high GFP were observed microscopically or by flow cytometry.

A representative experiment, using the mitochondrial Kgd1p:GFP, revealed that cells in the NQ fraction with high levels of Kgd1p:GFP were similar in viability and colony-forming units (CFUs) to Q cells (Figure 5), consistent with the Cit1p:GFP results above. In contrast, cells with low GFP and high ROS showed significant reduction in CFUs, typical of NQ cells. Finally, cells containing low GFP and low ROS exhibited an intermediate loss of reproductive or colony-forming capacity. We conclude that, while high ROS correlates with significant loss of reproductive capacity in NQ cells, because cells that are low GFP and low ROS also exhibit loss of reproductive capacity, this phenotype is not due simply to ROS accumulation. The production of petite colonies, indicative of mitochondrial mutations, exhibited a similar pattern in the three GFP/ROS populations. High-GFP, low-ROS cells produced few petite colonies whereas low-GFP, high-ROS and low-GFP, low-ROS cells were similar in numbers of petites (see Supplemental Material). Conclusions from these results are that the NQ fraction is heterogeneous, loss of reproductive capacity does not correlate absolutely with high ROS, and cells with characteristics of Q cells are present in the NQ or less-dense fraction.

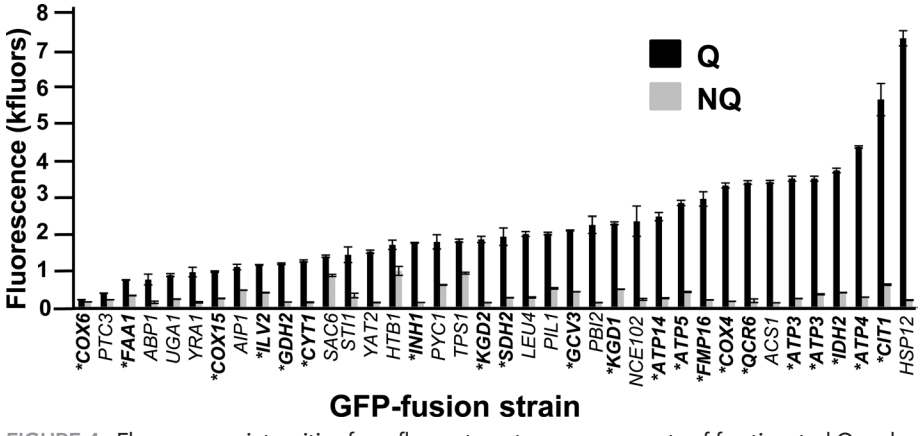

FIGURE 4: Fluorescence intensities from flow-cytometry measurements of fractionated Q and NQ populations from 38 GFP fusion strains. *Genes encoding proteins uniquely localized to mitochondria.

Because there were significant differences in mitochondrial GFP-fusion protein abundance between Q and NQ cell fractions, it was important to determine whether there were significant differences in respiration between the cell fractions. Respiration for each sample was measured in its respective medium, which is carbon depleted in SP cultures (Lillie and Pringle, 1980). We found that SP cultures, assayed in their own

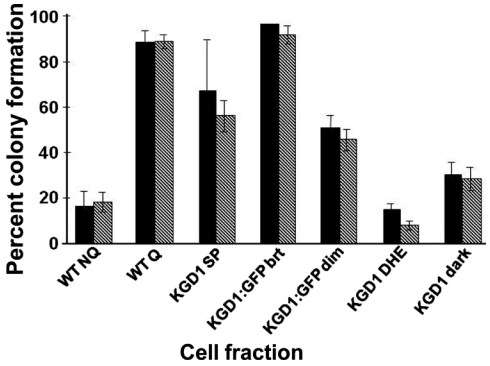

FIGURE 5: Reproductive capability as measured by CFUs for biological replicates of wild-type (S288c), NQ, and Q fractions and Kgd1p:GFP fusion strains sorted into GFP bright, DHE bright, and GFP DHE dim. There were no GFP and DHE bright cells.

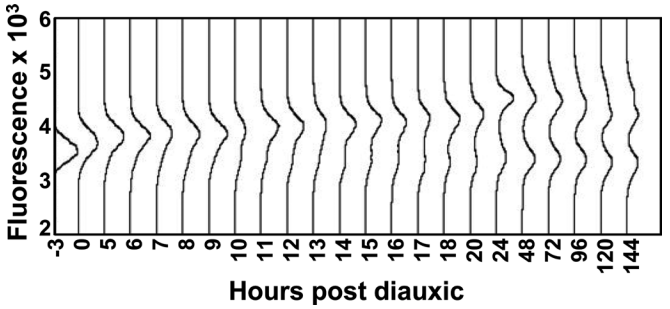

FIGURE 7: Flow-cytometry analysis of Cit1p:GFP fluorescence intensity as a function of time after glucose exhaustion in postdiauxic phase cultures. The *x*-axis is not to scale. Peaks represent number of events with a specific fluorescence intensity.

medium, respired at a rate 63% of that for EXP cultures (Figure 6). In contrast, Q cells had respiration rates 6 times higher than the NQ fraction ($p \leq 5.5 \times 10^{-6}$) and 1.6 times more than EXP cultures. We conclude from that that most cells in the NQ fraction are unable to use the nonfermentable carbon sources available in the medium and that Q cells, while not dividing, maintain fully functional and active mitochondria.

Q and NQ populations diverge in the first 24 h after glucose exhaustion

To study the process of Q and NQ differentiation using GFP-fusion strains that distinguish Q and NQ fractions, we examined cultures producing the mitochondrial protein Cit1p:GFP by flow cytometry from 1 to 7 d after inoculation. During this time, the postdiauxic phase, nonfermentable carbon sources are still available and Q and NQ cells differentiate (Figure 7). Initially, Cit1p:GFP abundance increased in the whole population, shown by a shift in the single peak to higher fluorescence intensity during the period from 3 h before to 9 h after glucose exhaustion at the diauxic. By 10 h postdiauxic, a second, dimmer population appears. The second peak becomes larger, shifts to lower fluorescence intensity through the time course, and corresponds to cells from an NQ fraction. The high fluorescence-intensity peak (Q cells) continues to increase in fluorescence, reaching a maximum at 24 h postdiauxic. We conclude from this time course data that both gain and loss of Cit1p:GFP are dynamic and differentiate Q and NQ populations between 14 and 20 h postdiauxic.

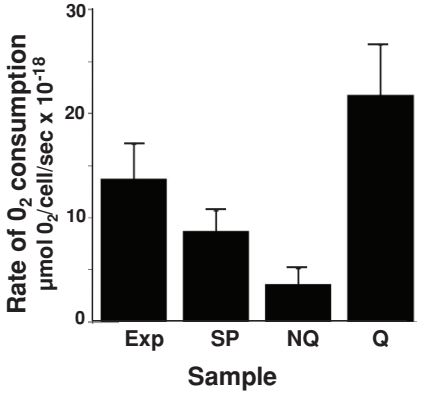

FIGURE 6: Oxygen consumption measurements of unfractionated EXP (13.7 µmol·cell·s) and SP (3.7 µmol·cell·s) and fractionated NQ (3.6 µmol·cell·s) and Q (21.8 µmol·cell·s) populations from S288c SP cultures. The difference between NQ and Q respiration is significant ($p \leq 5.5 \times 10^{-6}$).

Cit1p:GFP revealed two distinct populations with symmetry in protein abundance between dividing Q and NQ cells in the postdiauxic phase

We had assumed that the cell division after glucose exhaustion would lead to the formation of Q daughter cells and NQ cells and, thus, with respect to GFP expression, were expecting to see bright daughter and dim mother cells. To examine the cell division that occurs after glucose exhaustion, cells from cultures producing Cit1p:GFP or the nuclear protein Acs1p:GFP, both of which typically have bright Q cells and dim NQ cells, were studied at days 3, 5, and 7 after inoculation. In these cultures, ~40% of the NQ cells (less-dense fraction) were budded while none of cells in the more dense or Q fraction were budded. We discovered, at day 3, when mother:daughter relationships could be clearly determined, that essentially all mother:daughter pairs showed symmetry with respect to protein abundance (Figure 8). That is, bright, GFP-producing mothers gave rise to bright daughters and dim mothers gave rise to dim daughters. For Acs1p:GFP, symmetric protein expression

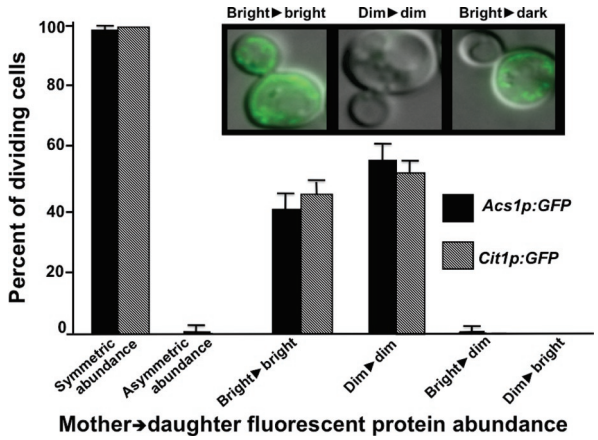

FIGURE 8. GFP protein expression in mother:daughter pairs 48 h after glucose exhaustion for two GFP fusion proteins: Cit1p:GFP and Acs1p:GFP. Insert: Examples of Cit1p:GFP bright mother ▶ bright daughter, dim mother ▶ dim daughter, bright mother ▶ dim daughter, and dim mother ▶ bright daughter. Bright mother ▶ dim daughter pairs were seen extremely rarely, and dim mother ▶ bright daughter, not at all. Symmetric and asymmetric abundance refers to whether mothers and daughters exhibit similar levels of GFP-fusion proteins.

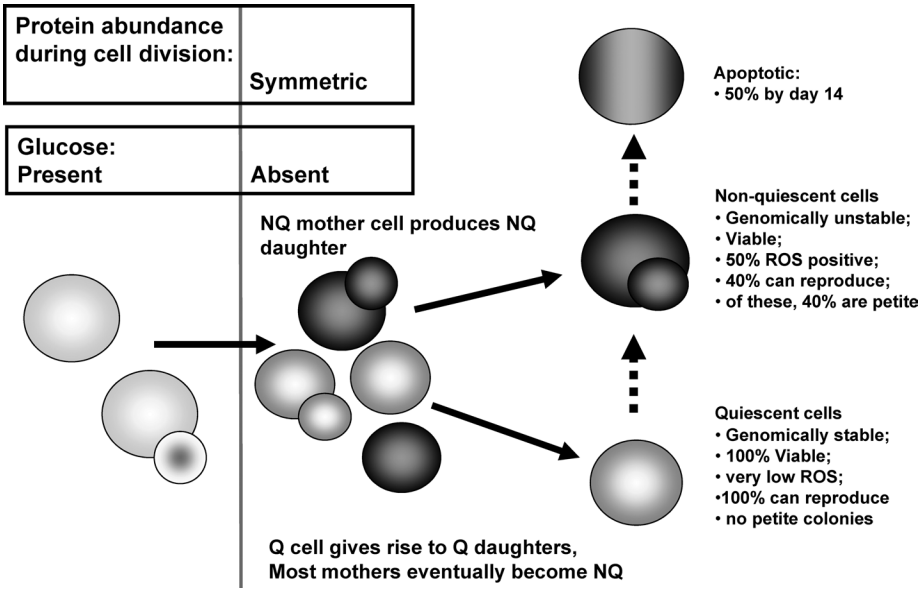

FIGURE 9: A model for cell differentiation in yeast cultures grown in rich, glucose-based medium (YPD) to SP. After glucose exhaustion the mother:daughter pairs exhibit symmetric distributions of GFP protein abundance with bright cells in the Q fractionated population and dim pairs in the NQ fraction. Dividing cells, both GFP expressing (Q) and dim (NQ), are predominantly in the less-dense fraction, consistent with the recent finding that density is a function of trehalose concentration (Shi *et al.*, 2010). Because most of the cells in the Q fraction are daughters, mother cells originally found in the Q fraction are hypothesized to become NQ cells.

during cell division was found 98.7% of the time (n = 228), and for Cit1p:GFP, symmetric protein expression during cell division was found 100% of the time (n = 209). Similar results were found for mother:daughter pairs on days 5 and 7 (see Supplemental Material). This result was surprising and led us to conclude that cells commit to becoming Q or NQ at or before glucose exhaustion.

Because most, but not all, dividing Q cells are in the less-dense fraction, and the denser Q fraction is 91% virgin daughters, most bright, Q-like mother cells must not be able to become dense again after division and would transition to NQ cells. Because both Q and NQ cells can be regrown to produce Q and NQ (mother and daughter) cells, we hypothesize that the cell-fate determinant is not due to mutation but is rather an epigenetic change that can be switched when cells that are able to divide are regrown. What controls this cell fate decision in yeast is not yet known.

DISCUSSION

High-throughput analysis of the 4159 strains in the yeast GFP-fusion library led to the identification of proteins, metabolic processes, and cell divisions that distinguish Q and NQ fractions in SP cultures. The utility of this library for understanding important biological processes should be obvious, and improvements in high-throughput flow cytometry and new technologies should make this library increasingly valuable.

As a result of this study, we have changed our model for the differentiation of Q and NQ cells (Figure 9). Our previous model predicted that the division *after* glucose exhaustion led to production of Q and NQ cells. Our current model shows cell-fate commitment occurring at or before the postdiauxic cell division, that is, during EXP. In the postdiauxic phase, cell fate is decided, and NQ mother cells produce NQ daughters and Q mother cells produce Q daughters. The ability to produce cells with distinct cell fates under one condition and like-daughters in another condition is reminiscent of divisions that allow maintenance, expansion, or extinction of stem cell populations (Tajbakhsh *et al.*, 2009). The new model leads to several testable hypotheses about the regulation and characteristics of Q/NQ cell differentiation.

There is potential bias in the GFP-fusion library (4159 strains) because it contains only the strains with relatively high levels of GFP expression during EXP; thus not all potential fusions are included (Huh *et al.*, 2003). Our finding that GFP-fusion proteins abundant in SP were typically not abundant in EXP is consistent with the hypothesis that some of the "missing" fusions might be abundant and important in SP. Of the 4159 GFP-fusion strains in the library, 4143 are still listed as genes by the Stanford Genome Database, leaving 2464 GFP fusions not in the library, including 1311 dubious or unverified genes. Of the remaining 1153 verified genes, GO Slim Mapper analysis revealed an overenrichment in the library for proteins with no known function, which tend to be found in high abundance in gene lists associated with SP and, especially, Q cells (Aragon *et al.*, 2008). Fortunately, the current library has enough diversity to provide significant insight into relatively unstudied states, such as SP.

This study identified several paradoxes, including 1) the development of metabolically distinct, relatively stable cell types in the same culture of a single-celled organism; 2) the inability of NQ cells to use the only carbon sources in their medium; and 3) high metabolic/respiratory activity in cells that appear "quiescent." Distinct cell types in the same culture are observed under other conditions, including sporulation, but, to our knowledge, unsporulated diploids have not been studied. We suspect that heterogeneity has been overlooked under many growth conditions and that this heterogeneity is likely to be critical for species survival and can provide important insights into development in tissue-complex eukaryotes.

One of the most puzzling observations is that NQ cells, as they are dividing, cannot use the only external carbon source available to them. Under these conditions, NQ cell survival requires that they metabolize their internal glycogen and trehalose stores and induce autophagy. The absence of glycogen in these cells and the

observation of autophagic vesicles (Allen *et al.*, 2006) are consistent with this hypothesis. In this condition, NQ cells would not compete for resources with Q cells and could produce nonfermentable substrates for Q cell respiration and survival. Thus the "viable but unculturable" NQ cells would also act as longer-term storage reserves for Q cells. We hypothesize that NQ cells are unable to down-regulate progrowth signaling pathways leading to programmed cell death, observed at 14 d, in NQ cells (Allen *et al.*, 2006). Clearly, this situation is complex and likely to provide many more biological insights relevant to single- and multicellular organisms.

Finally, while it was surprising for us to find that Q cells exhibit high rates of respiration, analysis of mitochondrial mutants suggests that the high respiration is required for maintenance of redox potentials and pools of NAD^+ and $NADP^+$ (Dodson, unpublished data). The significance of mitochondrial function for survival in Q cells has been shown previously (Martinez *et al.*, 2004; Aragon *et al.*, 2008), including the importance of genes like *CIT1* and *ATP1*, *2*, and *3* for SP survival. Additionally, chronological aging studies have shown that mitochondrial dysfunction leads to reduced survival in SP cultures (Aerts *et al.*, 2009; Fabrizio *et al.*, 2010). Interestingly, high rates of respiration in the absence of cell division and metabolic differences linked to maintenance of NADPH pools were recently reported in fibroblast stem cells (Lemons *et al.*, 2010). These results suggest that decreased respiration is not always a characteristic of the Q state and, in fact, may be necessary for survival of Q cells.

We have studied the process of entry into SP in rich, glucose medium (yeast peptone dextrose [YPD]), in which yeast survive for years, and questioned whether other conditions might elicit this differentiation. A study of yeast grown in high-glucose concentrations (700 g/l) showed cells enter an uncoupling phase allowing fermentation without growth and uncoupled cultures develop two cell populations, similar to Q and NQ cells (Benbadis *et al.*, 2009). Like Q cells, denser cells grown in high glucose exhibit higher respiration than the less-dense fraction. However, many of these cells have buds, and about half of the dense cells are dead. Another recent study showed differentiation of Q cells under constant low-glucose conditions (Shi *et al.*, 2010). The observation of a dense band of Q cells under conditions of constant high and low glucose provides strong support to the hypothesis that the signal for differentiation occurs before glucose exhaustion.

Other processes relevant to studies of SP include metabolic cycling, studied with chemostat cultures under low-glucose conditions (Tu *et al.*, 2005; Futcher, 2006; Shi *et al.*, 2010). Metabolic cycling is related to the differentiation of Q and NQ cells, in that a fraction of cycling cells exhibit increased density and high respiration when in the G_1 state. However, only specific strains exhibit cycling, and the cells of strains that can cycle do not form a stable band of Q cells in SP (Shi *et al.*, 2010). In contrast, S288c cells (the wild-type cells used in our studies) do not cycle well and have relatively stable Q and NQ populations in SP and under cycling conditions. Thus a comparative study of cycling and noncycling strains should be useful for identifying genes required for stability of Q cells and understanding the relationship between differentiation of Q cells and metabolic cycling.

Our studies of SP are relevant to chronological aging studied with SP cultures (Matecic *et al.*, 2010; Fabrizio and Longo, 2008). Because of the complexity of SP cultures, it is likely that genes found to lengthen or shorten culture survival may affect one or both cell types or communication between the two. The ability to follow different cell types in yeast SP cultures increases the value of this model system in studies of cell and tissue-level processes during aging and whether age-induced death of more complex organisms is the result of a discrete set of predictable, cell-specific events or cell–cell interactions.

MATERIALS AND METHODS

Growth conditions

For the GFP HyperCyt screen, individual strains from the Yeast GFP Fusion Localization Database (Huh *et al.*, 2003), constructed from the parental strain ATCC 201388: *MAT***a** *his3Δ1 leu2Δ0 met15Δ0 ura3Δ0* (S288C) (Brachmann *et al.*, 1998), were replicated into 96-well plates containing YPD + A (2% yeast extract, 1% peptone, 2% glucose, 0.04 mg/ml adenine) and 50 μg/ml ampicillin, using pin tools. The plates were covered with Breathe-Easy sealing membranes (Sigma Aldrich, St. Louis, MO, cat. #380059), and the strains were cultured at 30°C with aeration either overnight (for EXP) or for 7 d (for SP). For the 38-subpopulation strain analysis, wild-type (S288c) and the yeast GFP-fusion set (Huh *et al.*, 2003) were used for analysis. Strains were examined, single colonies were isolated on YPGal (to remove petites that accumulate in SP cultures), single colonies were obtained on YPD plates, and cells were cultured in liquid YPD + A (2% yeast extract, 1% peptone, 2% glucose, 0.04 mg/ml adenine, and 50 μg/ml ampicillin) at 30°C overnight for EXP and 7 d for SP samples.

Cell separation and harvest

To separate Q and NQ cells, Percoll (GE Healthcare, Piscataway, NJ) density gradients were made using a solution of one part 1.5 M NaCl per eight parts Percoll (vol/vol) (Allen *et al.*, 2006). The gradients were formed using 10-ml aliquots of this solution in 15-ml Corex tubes that were centrifuged at 24,700 × *g* for 15 min at 4°C in a Beckman Coulter (Fullerton, CA) JA-17 rotor. For separations, 5-ml samples of SP cultures were pelleted by centrifugation for 3 min at 3270 × *g* in a room-temperature Beckman Allegra tabletop centrifuge, resuspended in 500 μl 50 mM Tris-HCl buffer (pH 7.5), and overlaid onto the gradients, which were then centrifuged at 400 × *g* for 60 min at 25°C in a tabletop centrifuge with a swinging bucket rotor (Allegra X12-R, Beckman Coulter). After density-gradient centrifugation, the Q (dense) and NQ (less-dense) fractions were collected by pipette and pelleted by centrifugation in a microfuge, and each fraction was washed in 13 ml Tris buffer. The pellets were resuspended in 1 ml Tris buffer, and cells/ml were determined using a Z2 Coulter Counter (Beckman Coulter). The cells were again pelleted and then suspended in 100 μl of their own filter-sterilized, conditioned media for analysis.

High-throughput flow-cytometric screening

Three steps were used to prepare the samples for high-throughput screening. First, dilution plates were prepared by transferring 90 μl peptide dilution flow buffer (30 mM HEPES × ½ Na, 110 mM NaCl, 10 mM KCl, 1 mM $MgCl_2 \times 6H_2O$) into each well of the 384-well plates (Greiner Bio-One, Monroe, NC; cat. #781280) using the Biomek NX_{MC} (Beckman Coulter) liquid-handling robot. Second, 10 μl of each yeast strain was transferred from the 96-well growth plates into three adjacent wells of the 384-well dilution plates using the Biomek NX_{S8} (Beckman Coulter) liquid-handling robot. This step created a 1:10 dilution and generated three technical replicates for each sample. The 4th, 8th, 12th, 16th, 20th, and 24th columns of the dilution plates did not contain samples, just buffer alone. These columns served as a wash well used between different samples to minimize sample carryover. Third, the cells were sampled with a HyperCyt autosampler (Edwards *et al.*, 2004) controlled by HyperSip software and interrogated for GFP fluorescence with a CyAn ADP (DakoCytomation, Ft. Collins, CO)

flow cytometer using excitation at 488 nm and collection of fluorescent emissions with a 530/40-nm filter set. The data were processed using IDLeQuery software (Young *et al.*, 2005), and the median channel fluorescence for each sample was calculated and used for subsequent analyses.

Low-throughput flow cytometry and MoFlo-based cell sorting for reproductive capacity (CFUs)

For reanalysis of the 38 strains and Q/NQ fractions, ~5×10^6 cells were suspended in 500 µl filter-sterilized (0.22-µm pore size) Tris buffer in 2-ml flow tubes. These were analyzed for GFP fluorescence intensity using the Accuri C6 Flow Cytometer with the FL-1 channel. A total of 30,000 events were acquired for each of three technical replicates. Data were analyzed with IDLeQuery software (Young *et al.*, 2005). For fluorescence-activated cell sorting–enabled positioning of cells, samples were sorted using the MoFlo cell sorter (Beckman Coulter). For each sample, 144 cells (e.g., high GFP/low ROS, high ROS/low GFP, and low GFP/low ROS or Q cells and NQ cells) were positioned on solid YPD medium. At least three plates of 144 cells were obtained per sorted sample and incubated for 2–3 d at 30°C. Values represent the mean ± 1 SD for each sample.

DHE assay for quantification of ROS

DHE stock solution (Invitrogen, Carlsbad, CA) was diluted 1:10 in phosphate-buffered saline (PBS) (Fluka, Milwaukee, WI) for a working solution. Approximately 1×10^8 S288c upper- and lower-fraction cells per sample were pelleted and resuspended in 100 µl filter-sterilized, conditioned medium (typically from the same culture). Then 1 µl DHE working solution was added to each sample and incubated for 6 min at room temperature in the dark. The samples were washed three times in PBS and diluted to 1×10^6 cells/ml in Isoton II (Beckman Coulter). Approximately 30,000 cells per sample were analyzed with a FACScan flow cytometer (Clontech Laboratories) using 488 nm excitation and collecting fluorescent emission with filters at 585/42 nm for FL-1 parameter.

Microscopy

The fluorescent images were obtained using an Axioskop 2 MOT Plus microscope (Carl Zeiss, Thornwood, NY). All of the images were taken with a 50-ms exposure time for the differential interference microscopy image, 2000-ms exposure time for the rhodamine filter to detect DHE staining, and 2000-ms and automatic exposure times for the fluorescein isothiocyanate filter to detect GFP. The automatic exposure image was acquired for the purpose of identifying localization of protein in case the protein expression was too bright or dim for clarity in the 2000-ms image. AxioVision 4.7 software was used to compile and analyze the images.

Rate of oxygen consumption assay

Rates of oxygen consumption were determined using the BD Oxygen Biosensor System (BD Biosciences), which is a 96-well plate containing a fluorophore that fluoresces in the absence of oxygen. Q and NQ fractions were separated as described earlier and diluted to a concentration of 1×10^8 cells/ml, and 200 µl was placed in each well and subsequently coated with mineral oil. Fluorescence was measured every minute for 1 h, using a microplate reader and SoftMax Pro software. Relative fluorescence at each time point was normalized to the average signal of three control wells containing conditioned medium. Normal fluorescence units were converted to ρO_2 using the following equation: $\rho O_2 = (DR/NRF - 1)/K_{sv}$, where DR (dynamic range) is the ratio of the signal at zero oxygen to the signal at ambient condition, calculated using 100 mM sodium sulfite in PBS buffer; NRF is the normalized relative fluorescence; and K_{sv} is the Stern–Volmer constant, calculated using the following equation and then converted to units of atm^{-1}: $K_{sv} = (DR - 1)/\rho O_{2A}$, where ρO_{2A} is the partial pressure of oxygen at ambient conditions. ρO_{2A} was calculated by multiplying the mole fraction of oxygen at ambient conditions (0.209) by the total pressure in Albuquerque, NM (85 kPa). The ρO_2 of each time point for each well was converted to moles of oxygen by dividing by Henry's constant (756.5133 atm·l/mol at 25°C for air) and multiplying by the volume (2×10^{-4}l). Rates were determined from the slope of the regression line for time(s) versus M O_2/cell. Final rates were calculated as M O_2/cell/s and represented as an average of three biological replicates.

Correlation-based reproducibility analysis comparing GFP measurements between laboratories

To determine laboratory-to-laboratory reproducibility, fluorescence intensities of exponentially growing cells from our laboratory were compared with those from Newman *et al.* (2006). After excluding proteins with no measurements in either data set, a total of 2735 proteins were compared between data sets. Abundances of these proteins were correlated using Spearman's correlation (0.6554), Pearson's correlation (0.91), and Pearson's correlation of Savage scores based on protein abundance (0.8290).

GO analysis

To obtain lists of genes for GO analysis, median fluorescence-intensity values for the three EXP and SP replicates were $\log_2$ transformed and averaged before computing SP/EXP ratios for each strain. For ratio values greater than 2, the GO terms were tabulated using the GO Term Finder Database (www.yeastgenome.org/cgi-bin/GO/goTermFinder.pl).

IDLeQuery analysis of high-throughput flow-cytometry data

HyperCyt measurements were analyzed with the flow-cytometry software IDLeQuery (Young *et al.*, 2005), provided by the University of New Mexico Flow Cytometry Facility. Raw count data were gated and binned for plotting. IDLeQuery was used to plot relative distributions of forward-scatter and side-scatter intensity (the latter were $\log_{10}$ transformed).

SDI algorithm

To identify GFP fusion strains having two fluorescence peaks, the SP side-scatter (SS) data set was divided into 100 bins; each bin was averaged to compute log-FI. The EXP side-scatter (SS) data set was similarly processed to yield log-SS. Then for each bin, Δlog-FI, the difference between SP and EXP log-FI, was computed for each of the three technical replicates. A regression of Δlog-FI (from the difference between SP and EXP) versus log-SS (from SP) was computed, and the median of the regression slope across the three replicates was used to compute the SDI measure. Near-zero SDI values indicate low correlation, which is suggestive of a single peak of fluorescence intensity in both samples. Higher SDI values occur when there is not a good overlap of peaks; either there are single, nonoverlapping peaks in both samples or there are two peaks in one sample. Evaluation of the highest 78 strains identified by SDI revealed that 71 (91%) were strains that exhibited one peak in EXP and two peaks in SP (unpublished data).

k-Means clustering–based two peak identification

To identify proteins with two fluorescence peaks, k-means (k = 20) clustering was performed on each data set using the ratio of side scatter to forward scatter. The average profile for each cluster was computed, followed by visual identification of clusters with broad or jagged profiles. This analysis identified one cluster of 80 SP samples and one cluster with 99 EXP samples.

ACKNOWLEDGMENTS

We thank Benjamin Tu and Linda Breeden for helpful discussions and Karlett Parra's laboratory for their help, especially Eli Weber. This work was supported by National Science Foundation (NSF) grant MCB-0092364 to M.W.W. and UNMCMD (MH084690) (to L.S.). R.M.J., P.H.T., M.R.W., A.E.D., and E.E.M were supported by National Institutes of Health (NIH) for Maximizing Student Diversity grant GM-060201. R.M.J. was also supported by NIH GM-0975149, and E.E.M. had further support under a Louis Stokes Alliance for Minority Participation Bridge to the Doctorate fellowship grant through NSF HRD-0832947. Sandia National Laboratories is a multiprogram laboratory operated by Sandia Corporation, a wholly owned subsidiary of Lockheed Martin Corporation, for the U.S. Department of Energy's National Nuclear Security Administration under contract DE-AC04-94AL85000.

REFERENCES

Aerts AM, Zabrocki P, Govaert G, Mathys J, Carmona-Gutierrez D, Madeo F, Winderickx J, Cammue BPA, Thevissen K (2009). Mitochondrial dysfunction leads to reduced chronological lifespan and increased apoptosis in yeast. FEBS Lett 583, 113–117.

Aguilera A (1986). Deletion of the phosphoglucose isomerase structural gene makes growth and sporulation glucose dependent in *Saccharomyces cerevisiae*. Mol Gen Genet 204, 310–316.

Allen C *et al.*(2006). Isolation of quiescent and nonquiescent cells from stationary-phase yeast cultures. J Cell Biol 174, 89–100.

Aragon AD, Quiñones GA, Thomas EV, Roy S, Werner-Washburne M (2006). Release of extraction-resistant mRNA in stationary-phase *Saccharomyces cerevisiae* produces a massive increase in transcript abundance in response to stress. Genome Biol 7, 403–407.

Aragon AD, Rodriguez AL, Meirelles O, Roy S, Davidson GS, Tapia PH, Allen C, Joe R, Benn D, Werner-Washburne M (2008). Characterization of differentiated quiescent and nonquiescent cells in yeast stationary-phase cultures. Mol Biol Cell 19, 1271–1280.

Auesukaree C, Damnernsawad A, Kruatrachue M, Pokethitiyook P, Boonchird C, Kaneko Y, Harashima S (2009). Genome-wide identification of genes involved in tolerance to various environmental stresses in S. cerevisiae. J Appl Genet 50, 301–310.

Bagnat M, Keranen S, Shevchenko A, Simons K (2000). Lipid rafts function in biosynthetic delivery of proteins to the cell surface in yeast. Proc Natl Acad Sci USA 97, 3254–3259.

Benbadis L, Cot M, Rigoulet M, Francois J (2009). Isolation of two cell populations from yeast during high-level alcoholic fermentation that resemble quiescent and nonquiescent cells from the stationary phase on glucose. Fems Yeast Res 9, 1172–1186.

Brachmann CB, Davies A, Cost GJ, Caputo E, Li JC, Hieter P, Boeke JD (1998). Designer deletion strains derived from *Saccharomyces cerevisiae* S288C: a useful set of strains and plasmids for PCR-mediated gene disruption and other applications. Yeast 14, 115–132.

Coyle S, Kroll E (2008). Starvation induces genomic rearrangements and starvation-resilient phenotypes in yeast. Mol Biol Evol 25, 310–318.

Deshaies RJ, Koch BD, Werner-Washburne M, Craig EA, Schekman R (1988). A subfamily of stress proteins facilitates translocation of secretory and mitochondrial precursor polypeptides. Nature 332, 800–805.

DeVirgilio C, Burckert N, Barth G, Neuhaus JM, Boller T, Wiemken A (1992). Cloning and disruption of a gene required for growth on acetate but not on ethanol: the acetyl-coenzyme-A synthetase gene of *Saccharomyces cerevisiae*. Yeast 8, 1043–1051.

Dickinson JR (1991). Biochemical and genetic studies on the function and relationship between the PGI1-encoded and CDC30-encoded phosphoglucose isomerase in *Saccharomyces cerevisiae*. J Gen Microbiol 137, 765–770.

Dunham MJ, Badrane H, Ferea T, Adams J, Brown PO, Rosenzweig F, Botstein D (2002). Characteristic genome rearrangements in experimental evolution of *Saccharomyces cerevisiae*. Proc Natl Acad Sci USA 99, 16144–16149.

Edwards BS, Oprea T, Prossnitz ER, Sklar LA (2004). Flow cytometry for high-throughput, high-content screening. Curr Opin Chem Biol 8, 392–398.

Fabrizio P, Hoon S, Shamalnasab M, Galbani A, Wei M, Giaever G, Nislow C, Longo VD (2010). Genome-wide screen in *Saccharomyces cerevisiae* identifies vacuolar protein sorting, autophagy, biosynthetic, and tRNA methylation genes involved in life span regulation. PLoS Genet 6, e1001024.

Fabrizio P, Longo VD (2008). Chronological aging-induced apoptosis in yeast. Biochim Biophys Acta 1783, 1280–1285.

Fuge EK, Braun EL, Werner-Washburne M (1994). Protein synthesis in long-term stationary-phase cultures of *Saccharomyces cerevisiae*. J Bact 176, 5802–5813.

Futcher B (2006). Metabolic cycle, cell cycle, and the finishing kick to Start. Genome Biol 7, 107.

Giaever G *et al.* (2002). Functional profiling of the *Saccharomyces cerevisiae* genome. Nature 418, 387–391.

Horton LE, James P, Craig EA, Hensold JO (2001). The yeast hsp70 homologue Ssa is required for translation and interacts with Sis1 and Pab1 on translating ribosomes. J Biol Chem 276, 14426–14433.

Huh W-K, Falvo JV, Gerke LC, Carroll AS, Howson RW, Weissman JS, O' Shea EK (2003). Global analysis of protein localization in budding yeast. Nature 425, 686–691.

Imai J *et al.* (2003). The molecular chaperone Hsp90 plays a role in the assembly and maintenance of the 26S proteasome. EMBO J 22, 3557–3567.

Izawa S, Maeda K, Miki T, Mano J, Inoue Y, Kimura A (1998). Importance of glucose-6-phosphate dehydrogenase in the adaptive response to hydrogen peroxide in *Saccharomyces cerevisiae*. Biochem J 330, 811–817.

Kaeberlein M, Kirkland KT, Fields S, Kennedy BK (2005). Genes determining yeast replicative life span in a long-lived genetic background. Mech Ageing Dev 126, 491–504.

Kim KS, Rosenkrantz MS, Guarente L (1986). *Saccharomyces cerevisiae* contains two functional citrate synthase genes. Mol Cell Biol 6, 1936–1942.

Lee J, Spector D, Godon C, Labarre J, Toledano MB (1999). A new antioxidant with alkyl hydroperoxide defense properties in yeast. J Biol Chem 274, 4537–4544.

Lemons JMS, Feng X-J, Bennett BD, Legesse-Miller A, Johnson LE, Raitman I, Pollina EA, Rabitz HA, Rabinowitz JD, Coller HA (2010). Quiescent fibroblasts exhibit high metabolic activity. PLoS Biol 8, e1000514.

Le Tallec B *et al.* (2007). 20S proteasome assembly is orchestrated by two distinct pairs of chaperones in yeast and in mammals. Mol Cell 27, 660–674.

Lewis K (2007). Persister cells, dormancy and infectious disease. Nat Rev Microbiol 5, 48–56.

Li L, Lu Y, Qin L-X, Bar-Joseph Z, Werner-Washburne M, Breeden LL (2009). Budding yeast SSD1-V regulates transcript levels of many longevity genes and extends chronological life span in purified quiescent cells. Mol Biol Cell 20, 3851–3864.

Li W, Dang YJ, Liu JO, Yu BA (2010). Structural and stereochemical requirements of the spiroketal group of hippuristanol for antiproliferative activity. Bioorg Med Chem 20, 3112–3115.

Li W, Sun L, Liang Q, Wang J, Mo W, Zhou B (2006). Yeast AMID homologue Ndi1p displays respiration-restricted apoptotic activity and is involved in chronological aging. Mol Biol Cell 17, 1802–1811.

Lillie SH, Pringle JR (1980). Reserve carbohydrate-metabolism in *Saccharomyces cerevisiae*: responses to nutrient limitation. J Bacteriol 143, 1384–1394.

Lindqvist L, Pelletier J (2009). Inhibitors of translation initiation as cancer therapeutics. Future Med Chem 1, 1709–1722.

Martinez MJ, Roy S, Archuletta AB, Wentzell PD, Anna-Arriola SS, Rodriguez AL, Aragon AD, Quiñones GA, Allen C, Werner-Washburne M (2004). Genomic analysis of stationary-phase and exit in *Saccharomyces cerevisiae*: gene expression and identification of novel essential genes. Mol Biol Cell 15, 5295–5305.

Matecic M, Smith DL, Pan XW, Maqani N, Bekiranov S, Boeke JD, Smith JS (2010). A microarray-based genetic screen for yeast chronological aging factors. PLoS Genet 6, e1000921.

McAlister L, Holland M (1982). Targeted deletion of a yeast enolase structural gene. Identification and isolation of yeast enolase isozymes. J Biol Chem 257, 7181–7188.
Newman JRS, Ghaemmaghami S, Ihmels J, Breslow DK, Noble M, DeRisi JL, Weissman JS (2006). Single-cell proteomic analysis of *S. cerevisiae* reveals the architecture of biological noise. Nature 441, 840–846.
Planta RJ, Mager WH (1998). The list of cytoplasmic ribosomal proteins of *Saccharomyces cerevisiae*. Yeast 14, 471–477.
Qin SL, Moldave K, McLaughlin CS (1987). Isolation of the yeast gene encoding elongation factor 3 for protein synthesis. J Biol Chem 262, 7802–7807.
Raser JM, O'Shea EK (2004). Control of stochasticity in eukaryotic gene expression. Science 304, 1811–1814.
Raser JM, O'Shea EK (2005). Noise in gene expression: origins, consequences, and control. Science 309, 2010–2013.
Reinders J, Zahedi RP, Pfanner N, Meisinger C, Sickmann A (2006). Toward the complete yeast mitochondrial proteome: multidimensional separation techniques for mitochondrial proteomics. J Proteome Res 5, 1543–1554.
Repetto B, Tzagoloff A (1989). Structure and regulation of *KGD1*, the structural gene for yeast α-ketoglutarate dehydrogenase. Mol Cell Biol 9, 2695–2705.
Sales K, Brandt W, Rumbak E, Lindsey G (2000). The LEA-like protein HSP 12 in *Saccharomyces cerevisiae* has a plasma membrane location and protects membranes against desiccation and ethanol-induced stress. Biochim Biophys Acta 1463, 267–278.
Schirmaier F, Philippsen P (1984). Identification of two genes coding for the translation elongation factor eF-1α of *S. cerevisiae*.. EMBO J 3, 3311–3315.
Segal SP, Dunckley T, Parker R (2006). Sbp1p affects translational repression and decapping in *Saccharomyces cerevisiae*. Mol Cell Biol 26, 5120–5130.
Shi L, Sutter B, Xinyue Y, Tu B (2010). Trehalose is a key determinant of the quiescent metabolic state that fuels cell cycle progression upon return to growth. Mol Biol Cell 21, 1982–1990.
Stevens TH, Forgac M (1997). Structure, function and regulation of the vacuolar (H^+)-ATPase. Annu Rev Cell Dev Biol 13, 779–808.
Suissa M, Suda K, Schatz G (1984). Isolation of the nuclear yeast genes for citrate synthase and 15 other mitochondrial proteins by a new screening method. EMBO J 3, 1773–1781.
Tajbakhsh S, Rocheteau P, Le Roux I (2009). Asymmetric cell divisions and asymmetric cell fates. Annu Rev Cell Dev Biol 25, 671–699.
Tu BP, Kudlicki A, Rowicka M, McKnight SL (2005). Logic of the yeast metabolic cycle: temporal compartmentalization of cellular processes. Science 310, 1152–1158.
Wright RM, Simpson SL, Lanoil BD (1995). Oxygen regulation of the cytochrome c oxidase subunit VI gene, *COX6*, in *Saccharomyces cerevisiae*.. Biochem Biophys Res Commun 216, 676–685.
Young SM, Bologa C, Prossnitz ER, Oprea TI, Sklar LA, Edwards BS (2005). High-throughput screening with HyperCyt® flow cytometry to detect small molecule formylpeptide receptor ligands. J Biomol Screen 10, 374–382.